Capacitance characteristics of phase separated $La_{0.5}Ca_{0.5}MnO_3/Nb-SrTiO_3$ *p-n* junction

B. T. Xie, Y. G. Zhao,[a)] and C. M. Xiong
Department of Physics and State Key Laboratory of New Ceramics and Fine Processing, Tsinghua University, Beijing 100084, People's Republic of China

(Received 3 July 2008; accepted 31 July 2008; published online 22 August 2008)

The capacitance characteristics of $La_{0.5}Ca_{0.5}MnO_3/Nb-SrTiO_3$ *p-n* junction and magnetic property have been investigated. The magnetic field-induced increase in *ferromagnetic metallic* phase, irreversibility, and the exchange bias effect were observed. The junction also shows a remarkable thermal hysteresis of capacitance, a giant positive magnetocapacitance (MC), a remarkable difference of MC for the zero field cooling and field cooling processes, and a memory effect of magnetic field. The results can be understood in terms of phase separation. This work demonstrates the remarkable tunability of the capacitance for phase separated manganite heterojunctions, which may have potential applications. © *2008 American Institute of Physics*. [DOI: 10.1063/1.2973904]

The perovskite manganite-based junctions have been intensively investigated recently because of their good rectifying characteristics,[1–5] remarkable magnetoresistance,[2] and magnetocapacitance (MC).[4,5] In manganites, charge, spin, lattice, and orbital degrees of freedoms are strongly coupled, leading to various ground states and rich phase diagram.[6] Recent studies suggest phase separation (PS) in perovskite manganite, typically involving ferromagnetic metallic (FM) and antiferromagnetic charge and orbital ordered (COAFM) insulating domains.[7] PS, which can be tuned by various factors, is absent in the traditional semiconductor *p-n* junctions, so it is interesting to study the phase separated manganite *p-n* junctions and related physics. However, the work on PS related behavior of *p-n* junctions based on phase separated manganites is rather limited.[8]

Half-doped manganite $La_{0.5}Ca_{0.5}MnO_3$ (LCMO) has been widely studied as a prototypical PS manganite and the coexistence of the FM and COAFM phases in a wide temperature range was observed.[9] In our previous work,[8] the current-voltage (*I-V*) characteristics of the $La_{0.5}Ca_{0.5}MnO_3/Nb-SrTiO_3$ junctions were studied and some interesting behaviors related to PS were observed. For traditional semiconductor *p-n* junctions, capacitance has been proved to be a very useful tool in their studies.[10] Unfortunately, the studies on the capacitance of manganite-based *p-n* junctions are limited[3–5,11] and the PS related capacitance behavior has not been reported yet. On the other hand, the coexistence of magnetic and nonmagnetic phases in LCMO has been demonstrated in $La_{0.5}Ca_{0.5}MnO_3$ thin films by magnetic force microscopy (MFM);[8] however, the nature of the nonmagnetic region cannot be determined by MFM. So, further study on the magnetic property of LCMO thin film is needed.

In this letter, the capacitance characteristics and magnetic property of $La_{0.5}Ca_{0.5}MnO_3/Nb-SrTiO_3$ *p-n* junction are studied. A remarkable thermal hysteresis of capacitance, a giant positive MC, a remarkable difference of MC for the zero field cooling (ZFC) and field cooling (FC) processes, and a memory effect of magnetic field are observed in this junction. Magnetic field-induced increase in FM regions and the exchange bias effect were observed. The capacitance characteristics of $La_{0.5}Ca_{0.5}MnO_3/Nb-SrTiO_3$ junction are explained by considering the PS in LCMO.

The details of sample fabrication and electrode configuration were described elsewhere.[8] The magnetic property of LCMO films was measured by using a Quantum Design magnetic property measurement system (MPMS XL7). The capacitance of the junction was measured by an *LCR* meter ZM2353 with the low temperature and magnetic field of MPMS. The *C-V* curves were measured at a frequency of 10 kHz.

Since the coexistence of the FM and COAFM phases in a wide temperature range was observed in LCMO bulk samples,[9] it is expected that the nonmagnetic region in the MFM images of the LCMO thin film is the AFM phase. In this case, the exchange bias effect may be observed in the LCMO film. Figure 1(a) shows the ZFC and FC *M-H* loops, respectively. The inset displays the expanded view of the central part of the *M-H* loops. Compared to the ZFC *M-H* loop, the *M-H* loop with $\mu_0H=0.1$ T FC from 300 to 10 K

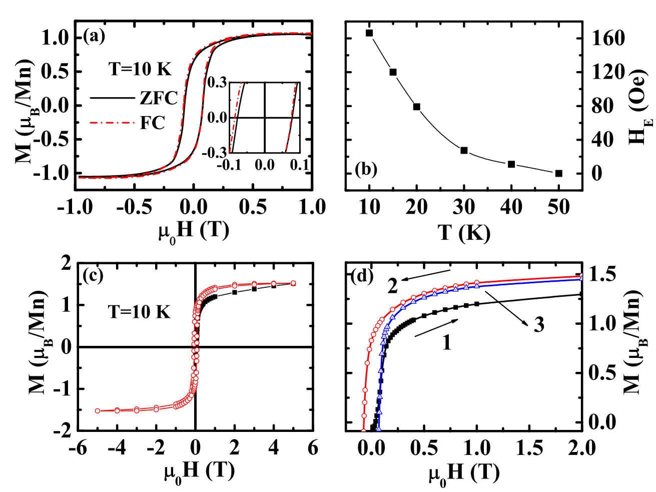

FIG. 1. (Color online) (a) *M-H* loops of the LCMO film at 10 K for ZFC and FC under $\mu_0H=0.1$ T from 300 K. (b) Temperature dependence of the exchange bias field H_E. (c) *M-H* curve of the junction at 10 K. (d) The expanded view of the *M-H* curve including the initial magnetization curve. Inset of (a) is the enlargement of the central part of the *M-H* loops.

[a)]Electronic mail: ygzhao@tsinghua.edu.cn.

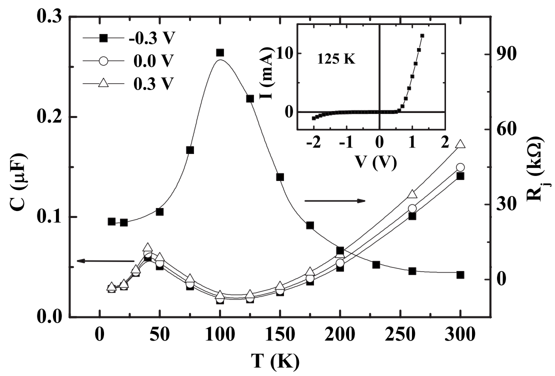

FIG. 2. Temperature dependence of capacitance and resistance of the junction at selected bias voltages. Inset is the current-voltage curve at 125 K.

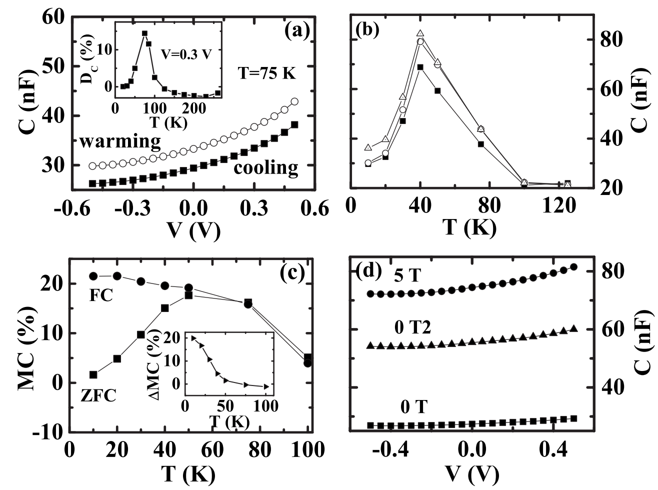

FIG. 3. (a) C-V curves measured at 75 K in the cooling and warming processes, respectively. (b) Temperature dependence of capacitance at the bias voltage of 0.3 V measured in the warming process with $\mu_0 H=0$ T after ZFC (filled squares) and $\mu_0 H=0.2$ T after ZFC (open circles) and FC (open triangles). (c) MC vs temperature for FC and ZFC calculated from (b). (d) C-V curves of the junction with $\mu_0 H=0$, 5.0, and 0 T successively. Inset of (a) is the capacitance difference, D_C, between the cooling and warming measurements at $V=0.3$ V. Inset of (c) shows the temperature dependence of $\Delta\mathrm{MC}=\mathrm{MC}_{\mathrm{FC}}-\mathrm{MC}_{\mathrm{ZFC}}$.

shows a significant exchange bias field $H_E=166$ Oe at 10 K with $H_E=-(H_{C1}+H_{C2})/2$, where H_{C1} and H_{C2} are the left and right coercive fields, respectively. The exchange bias effect has been well established for FM/AFM or FM/spin glass structures.[12] Considering the coexistence of FM and COAFM phases in LCMO bulk samples,[9] it is reasonable to deduce that the nonmagnetic region in the LCMO film is the AFM phase. The temperature dependence of H_E is exhibited in Fig. 1(b), which shows that the value of H_E decreases with increasing temperature and vanishes at about $T=50$ K, denoted as the "blocking" temperature T_B.[12]

The magnetic hysteresis of the LCMO film was measured between −5.0 and 5.0 T after ZFC from 300 to 10 K and the result is depicted in Fig. 1(c) with the expanded view shown in Fig. 1(d). Unlike the magnetic hysteresis loops of the conventional ferromagnet, the initial magnetization curve (black, curve "1") does not lie between the field descending curve (red, curve "2") and the field ascending curve (blue, curve "3") but much lower than the latter two. This phenomenon indicates that the FM regions increase upon applying a 5.0 T magnetic field due to the transformation of COAFM phase to FM phase and this change persists when the magnetic field decreases. So, transformation between the COAFM and FM phases is irreversible.

Figure 2 is the temperature dependence of capacitance (C-T) at three bias voltages and the junction resistance (R_j-T) at the bias voltage of −0.3 V, where $R_j \equiv V/I$. The inset of Fig. 2 is the I-V curve of LCMO/NSTO junction, which shows the rectifying characteristic. With decreasing temperature, the capacitance decreases and reaches a minimum at about 100 K, which is consistent with the temperature of R_j peak, and then increases to show a peak near 50 K. According to the parallel panel capacitor model, the capacitance of the junction can be expressed as $C=\varepsilon_0\varepsilon_r S/d$, where ε_r is the permittivity, S is the effective electrode area, and d is the thickness of the dielectric layer between the two electrodes. For LCMO/NSTO junction, the depletion layer can be considered as the dielectric layer. Since the thickness of the depletion layer is roughly proportional to $V_D^{1/2}$ (Ref. 10), where V_D is the diffusion potential, and V_D increases with decreasing temperature,[8] the increase in the junction resistance R_j and the decrease in the junction capacitance with decreasing temperature from 300 to 100 K can be understood. The temperature dependence of magnetization for the sample shown in Fig. 2(c) of Ref. 8 suggests that the amount of the FM phase is small at high temperatures (300–100 K) and increases remarkably at low temperatures (<100 K). Therefore, at low temperatures, the remarkable increase in FM regions favors the decrease in R_j and the increase in capacitance. When the effect of the FM region increase overwhelms the effect of V_D, the decrease in R_j and the increase in capacitance will occur. For the origin of the capacitance peak near 50 K, it is likely to be related to the dielectric constant of the depletion layer of NSTO since ε_r-T curve of $SrTiO_3$ shows a peak near 50 K.[13] Actually, a similar peak near 50 K is presented in the C-T curves of $La_{0.67}Sr_{0.33}MnO_{3-\delta}$/Nb:$SrTiO_3$ (Ref. 3) and $Nd_{0.5}Sr_{0.5}MnO_3$/Nb:$SrTiO_3$ (Ref. 5). This lends further support to the explanation of the peak since the property of manganites in our work and those in Refs. 3 and 5 are quite different.

The C-V curves at different temperatures depend on the thermal history and show remarkable thermal hysteresis behavior at low temperatures. The capacitance values measured in the warming process (C_W) are larger than those in the cooling process (C_C) under the same bias voltage, as shown in Fig. 3(a). This effect is most remarkable at 75 K. The difference between the two processes at the bias of $V=0.3$ V, defined as $D_C=(C_W-C_C)/C_C\times 100\%$, is depicted in the inset of Fig. 3(a). D_C shows a peak at 75 K and approaches zero within experimental error in the low and high temperature regimes. This thermal hysteresis effect originates from the first order transition between FM and COAFM phases.[14]

The junction capacitance can also be tuned by magnetic field and shows positive MC. The C-V curves of the junction were measured at selected temperatures in the warming process, with or without magnetic field. The C-V curves of the junction were measured under $\mu_0 H=0$ T after ZFC, $\mu_0 H=0.2$ T after ZFC, and $\mu_0 H=0.2$ T after FC, respectively. We selected the capacitance at bias voltage $V=0.3$ V in each C-V curve with the three measurements described above and plotted the C-T curves in Fig. 3(b). The three C-T curves are nearly identical above 100 K, i.e., no evident MC effect, but discrepant with each other below 100 K. The MC values were calculated as $MC=[C(0.2\ T)-C(0\ T)]/C(0\ T)\times 100\%$ from the data in Fig. 3(b) and the temperature dependence of MC is shown in Fig. 3(c). The MC for the FC process (MC_{FC}) is larger than that of the ZFC process (MC_{ZFC}) and the difference between them increases with the decrease in temperature, as shown in the inset of Fig. 3(c). This behavior will be discussed later.

The *C-V* curves were also measured at 10 K under $\mu_0 H=0$, 5.0 T, and removal of the magnetic field (0 T2) successively. The result is shown in Fig. 3(d). With a 5.0 T magnetic field, the capacitance of the junction is enhanced remarkably and MC reaches 170%. After the removal of the magnetic field, the capacitance decreases but is still larger than its initial value, indicating that the capacitance of the junction shows a magnetic memory effect. This memory effect can be explained by considering the PS in the LCMO film. As shown in Fig. 1(d), the FM regions in LCMO increase upon applying a 5.0 T magnetic field and cannot convert to the COAFM phase completely with decreasing field. At low temperatures, the junction is inhomogeneous and can be regarded as a capacitor with COAFM and FM regions in the LCMO film alternately contacting with the NSTO substrate. Since the COAFM regions are insulating and FM regions are more conducting, the increase in FM regions makes the effective electrode area *S* larger, resulting in the increase in the effective capacitance of the junction. The total effective capacitance of the LCMO/NSTO junction is mainly determined by the FM regions in LCMO near the interface. So the persistence of FM regions after the removal of the magnetic field can account for the magnetic memory effect of the junction capacitance. This scenario can also account for the difference between MC_{FC} and MC_{ZFC} shown in Fig. 3(c). The FM regions induced by magnetic field in the FC process are larger than that in the ZFC process at low temperatures and this difference enhances with decreasing temperature, resulting in the larger MC_{FC} and the temperature dependence of $\Delta MC=MC_{FC}-MC_{ZFC}$.

It should be emphasized that the phase separated manganite junctions show giant MC due to the tuning of PS by magnetic field. This mechanism is quite different from those based on the magnetic field-induced reduction in the effective depletion width of $La_{0.67}Sr_{0.33}MnO_{3-\delta}/Nb:SrTiO_3$ (Ref. 4) or the increase in the effective carrier concentration in $Nd_{0.5}Sr_{0.5}MnO_3/Nb:SrTiO_3$ (Ref. 5). For our phase separated LCMO/NSTO junction, MC can reach 170% at $T=10$ K with $\mu_0 H=5$ T, much larger than those reported by Nakagawa *et al.*[4] ($MC\approx 33\%$, $T=10$ K, $\mu_0 H=8$ T) and Matsuno *et al.*[5] ($MC\approx 26\%$, $T=5$ K, $\mu_0 H=7$ T), suggesting the advantage of phase separated manganite *p-n* junctions in getting giant MC.

In summary, the magnetic properties of the LCMO film and the capacitance characteristics of the $La_{0.5}Ca_{0.5}MnO_3/Nb-SrTiO_3$ junction have been studied. The magnetic field-induced increase in FM regions, irreversibility, and the exchange bias effect were observed. A remarkable thermal hysteresis of capacitance, a giant positive MC, a remarkable difference of MC for the ZFC and FC processes, and a memory effect of the magnetic field were present in this junction. PS scenario was used to account for the results. This work demonstrates that the capacitance of phase separated manganite junctions shows various interesting behaviors, which may have potential applications.

This work was supported by the National Science Foundation of China (Grant Nos. 50425205 and 10674079) and National 973 project (Grant No. 2006CB921502).

[1] M. Sugiura, K. Uragou, M. Noda, M. Tachiki, and T. Kobayashi, Jpn. J. Appl. Phys., Part 1 **38**, 2675 (1999); H. Tanaka, J. Zhang, and T. Kawai, Phys. Rev. Lett. **88**, 027204 (2002); H. B. Lu, S. Y. Dai, Z. H. Chen, L. Yan, Y. L. Zhou, and G. Z. Yang, Chin. Sci. Bull. **48**, 1328 (2003).
[2] J. R. Sun, C. M. Xiong, T. Y. Zhao, S. Y. Zhang, Y. F. Chen, and B. G. Shen, Appl. Phys. Lett. **84**, 1528 (2004); P. L. Lang, Y. G. Zhao, B. Yang, X. L. Zhang, J. Li, P. Wang, and D. N. Zheng, *ibid.* **87**, 053502 (2005); K. J. Jin, H. B. Lu, Q. L. Zhou, K. Zhao, B. L. Cheng, Z. H. Chen, Y. L. Zhou, and G. Z. Yang, Phys. Rev. B **71**, 184428 (2005).
[3] T. Susaki, N. Nakagawa, and H. Y. Hwang, Phys. Rev. B **75**, 104409 (2007).
[4] N. Nakagawa, M. Asai, Y. Mukunoki, T. Susaki, and H. Y. Hwang, Appl. Phys. Lett. **86**, 082504 (2005).
[5] J. Matsuno, A. Sawa, M. Kawasaki, and Y. Tokura1, Appl. Phys. Lett. **92**, 122104 (2008).
[6] P. Schiffer, A. P. Ramirez, W. Bao, and S.-W. Cheong, Phys. Rev. Lett. **75**, 3336 (1995).
[7] E. Dagotto, T. Hotta, and A. Moreo, Phys. Rep. **344**, 1 (2001).
[8] B. T. Xie, Y. G. Zhao, C. M. Xiong, S. Park, and W. Wu, Appl. Phys. Lett. **92**, 232109 (2008).
[9] G. Allodi, R. De Renzi, F. Licci, and M. W. Pieter, Phys. Rev. Lett. **81**, 4736 (1998); J. C. Loudon, N. D. Mathur, and P. A. Midgley, Nature (London) **420**, 797 (2002).
[10] S. M. Sze, *Physics of Semiconductor Devices*, 2nd ed. (Wiley, New York, 1981).
[11] A. Sawa, A. Yamamoto, H. Yamada, T. Fujii, M. Kawasaki, J. Matsuno, and Y. Tokura, Appl. Phys. Lett. **90**, 252102 (2007).
[12] J. Nogués, J. Sort, V. Langlais, V. Skumryev, S. Surinach, J. S. Munoz, and M. D. Baró, Phys. Rep. **422**, 65 (2005).
[13] H.-M. Christen, J. Mannhart, E. J. Williams, and Ch. Gerber, Phys. Rev. B **49**, 12095 (1994).
[14] Y. M. Xiong, G. Y. Wang, X. G. Luo, C. H. Wang, X. H. Chen, X. Chen, and C. L. Chen, J. Appl. Phys. **97**, 083909 (2005).